Article

J. Biol. Regul. Homeost. Agents. 2024; 38(6): 4743–4755
https://doi.org/10.23812/j.biol.regul.homeost.agents.20243806.379

Sodium Aescinate Alleviates Diabetic Retinopathy in Rats by Inhibiting the AGE-RAGE Signaling Pathway

Shule Jiang[1], Yun Cao[2,*]

[1]Department of Ophthalmology, The First Affiliated Hospital of Zhejiang Chinese Medical University (Zhejiang Provincial Hospital of Chinese Medicine), 310006 Hangzhou, Zhejiang, China
[2]Department of Endocrinology, The First Affiliated Hospital of Zhejiang Chinese Medical University (Zhejiang Provincial Hospital of Chinese Medicine), 310006 Hangzhou, Zhejiang, China
*Correspondence: caoyun2024@163.com (Yun Cao)
Submitted: 9 November 2023 Revised: 30 December 2023 Accepted: 4 January 2024 Published: 1 June 2024

Background: Diabetic retinopathy (DR) is a complication of diabetes that impacts the vision and quality of life of patients. Sodium aescinate (SA) has been widely used in resisting exudation and treating inflammation and vascular diseases, which is consistent with the disease symptoms of DR. However, the therapeutic effect and molecular mechanism of SA on DR are lacking. Therefore, this study is aimed at examining the palliative impact of SA on DR rats induced by streptozotocin (STZ).
Methods: DR model was established by injecting STZ (80 mg/kg) into the Sprague Dawley (SD) rats (7-week-old). Later, SA was administered via the tail vein at a dosage of 1 mg/kg/per, 7 days/cycle, totaling 21 days. During this period, the changes in the rats' body weight and blood sugar levels were observed, and their glucose tolerance was monitored. The fundus conditions of the rats were then examined using fundus photography, focusing on the diameter and permeability of blood vessels. Retinal pathology was assessed using hematoxylin-eosin (HE) staining, and the changes in DR-related markers vascular endothelial growth factor (VEGF) and tumor necrosis factor-α (TNF-α) in the retinas were assayed. The changes in reactive oxygen species (ROS), lipid peroxidation (Lip-ROS), malondialdehyde (MDA), glutathione (GSH), and insulin-like growth factor 1 (IGF1) in retinal protein, as well as the changes of IGF1 in the serum, were also evaluated. Additionally, the changes in the advanced glycation end products (AGE)-receptor for AGEs (RAGE) signaling pathway were investigated.
Results: The treatment group with SA slowed down the diameter of fundus blood vessels and reduced angiogenesis in DR. It inhibited the expression of VEGF and TNF-α. At the same time, SA could also inhibit the activation of ROS, MDA, GSH, and IGF1, and reduce the protein content of IGF1. Additionally, the expression of AGE and RAGE in the advanced glycation end products (AGE)-receptor for AGEs (RAGE) signaling pathway was decreased, and the phosphorylated Janus kinase-signal transd ucer and activator of transcription 3 (JAK/STAT3) in its downstream pathway was also downregulated.
Conclusions: SA has the capacity to diminish DR by inhibiting oxidative stress and AGE-RAGE signaling pathway.

Keywords: DR; SA; ROS; AGE-RAGE signaling pathway

Introduction

The Global Diabetes Data 2021 report indicated that there are over 537 million people worldwide with diabetes, a metabolic disease, and this number is expected to continue rising in the future [International Diabetes Federation (IDF), https://diabetesatlas.org/]. One of the complications of diabetes mellitus (DM) is diabetic retinopathy (DR), a condition where chronic vascular lesions can result in retinal damage [1]. In terms of DR, retinal microvascular injury plays a significant role [2]. DR has two classifications: non-proliferative and proliferative, both of which are associated with microvascular disease [3,4]. The development of DR coincides with the progression of DM, with more than one-third of people with diabetes also experiencing DR [5], highlighting the global burden of the condition. As a result, our research focuses on preventing the occurrence and progression of DR.

Microvascular injury in diabetic retinopathy (DR) involves several key mechanisms. The aberration of vascular endothelial growth factor (VEGF) a significant signal [6]. Elevated levels of VEGF in DR lead to signaling in endothelial cells, causing changes in vascular permeability and promoting neovascularization. The introduction of anti-VEGF treatment has shown promise in improving vision and preventing or reversing neovascularization, making it an important clinical treatment strategy (IDF, https://diabetesatlas.org/) [7]. Insulin-like growth factor 1 (IGF1) is another protein involved in the development of new blood vessels and has been implicated in retinal damage [8]. Additionally, IGF1 has been found to inhibit reactive oxygen species (ROS) and enhance the antioxidant capacity of cells, suggesting a protective role against oxidative stress [9]. Interestingly, elevated VEGF levels can trigger the generation of ROS. The discoveries underscore

Journal of
BIOLOGICAL REGULATORS
and Homeostatic Agents

the significance of VEGF and IGF1 in the onset and treatment of DR. Further research in these areas may lead to improved therapeutic strategies for preventing and managing this condition [10,11].

Numerous studies have revealed the critical role of ROS in the development of DR, particularly in microangiopathy complications [12]. High blood sugar levels contribute to oxidative stress and an imbalance in antioxidants. Interestingly, ROS activation can interfere with glucose metabolism, leading to mitochondrial dysfunction and influencing the development of DR microangiopathy [13–15]. ROS upregulation also triggers various pro-inflammatory pathways, causing phenotypic changes and the continued expression of pro-inflammatory genes, even after blood glucose levels stabilize. One example of this is the glycosylation of plasma proteins, such as insulin, under high glucose conditions. Glycosylated insulin can act as a ligand for the receptor for advanced glycation end products (RAGE), triggering the production of ROS and consequently leading to insulin resistance [16]. Similarly, the increased levels of ROS induced by high blood sugar levels can activate the advanced glycation end products (AGE)-receptor for AGEs (RAGE) signaling pathway [17]. But, the specific role of the AGE-RAGE signaling pathway in DR studies is still not entirely clear. Furthermore, the impaired regulation of ROS has been associated with metabolic abnormalities in diabetes, which can lead to complications such as DR [18]. These mechanisms involve an increased formation of advanced glycation end products (AGEs), increased expression of AGE receptors, and their activating ligands [19]. Investigating the correlation between the AGE-RAGE signaling pathway and DR is an intriguing prospect in the antioxidant study of DR and may provide further therapeutic insights.

Sodium aescinate (SA) is a sodium salt of triterpenoid saponins derived from the dried and mature seeds of *Aesculus wilsonii Rehd* [20]. SA has been extensively utilized in clinical settings to treat soft tissue swelling and venous edema, as it aids in reducing vascular permeability [21]. Recent studies have also demonstrated the remarkable anti-inflammatory and antioxidant properties of SA [22,23]. However, there has been limited research on the specific effects of SA on DR, which is associated with retinal edema, vascular abnormalities, and oxidative stress [24]. Our focus is on examining how SA can alleviate DR by regulating oxidative stress, aiming to shed light on the potential benefits of SA in mitigating the impact of DR and improving retinal health.

Materials and Methods

Materials

SA was purchased from Aimin Pharmaceutical Company (H20213782, Wuhan, China). Streptozotocin (STZ) (HY-13753) was obtained from MedChemExpress (Monmouth Junction, NJ, USA). Evans blue dye (EBD, E2129) was purchased from Sigma-Aldrich® (Saint Louis, MO, USA). The Glucose Test Kit (O-toluidine method, S0201S), ROS (S0033S), glutathione (GSH) (S0053) and malondialdehyde (MDA, S0131S) kit were obtained from the Beyotime Institute of Biotechnology (Shanghai, China). Rabbit anti-cell adhesion molecule-1 (CD31) (ab28364), anti-AGE (ab176173), anti-IGF1 (ab106836), anti-VEGFA (ab214424), anti-tumor necrosis factor-α (TNF-α) (ab6671), anti-phosphorylation-Janus kinase (p-JAK) (ab32101) and anti-RAGE (ab216329) antibodies were purchased from Abcam (Cambridge, MA, USA). Rabbit, anti-JAK (#3230), anti-STAT3 (#9139), anti-p-STAT3 (#9145), and anti-β-actin (#4967) antibodies were obtained from Cell Signaling Technologies (Danvers, MA, USA). Phosphate buffered saline (PBS, CB012), anti-rabbit IgG (LF104), anti-mouse IgG (LF103), Electrochemiluminescence detection reagents (SQ203L) and a bicinchoninic acid (BCA) protein assay kit (ZJ102L) was purchased from Epizyme Biotech (Shanghai, China).

Animals

Male-specific pathogen-free (SPF) Sprague-Dawley (SD) rats, 6 weeks of age, were acquired from Shanghai Slake Experimental Animal Co., Ltd. (Shanghai, China) and were housed in accordance with relevant guidelines. They underwent adaptive feeding for one week. The animal study was approved by the Ethics Committee for Animal Study in Animal Ethical and Welfare Committee of Zhejiang Chinese Medical University (approval number: IACUC-20230904-04). This experiment strictly follows the Regulations on the Management of Experimental Animals and other relevant provisions.

Animals' Experimental Protocols

SD rats were randomly divided into 5 groups: control group, DR Group, SA1-3 group (0.5/1.0/1.5 mg/kg), 6 rats/group. Control group was administered with a citric acid buffer of equal volume. DR-model group and SA-treat group were induced by a single injection of STZ (80 mg/kg). SA group was given intravenous SA (0.5/1.0/1.5 mg/kg/day), 7 days/cycle. Total of 21 days of treatment (According to the SA injection instructions, every 7 days for a course of treatment. There are 7 days between each session). The weight of the rats was measured per 7 days, and the blood glucose was measured after the experiment. Blood glucose was measured on the seventh day after the first STZ injection. DR-Rats were selected with blood glucose $>$16.5 mmol/L. In the DR group, less than 20 rats with unqualified blood glucose were injected with STZ again. Twenty rats were randomly divided into four cages (DR Group, SA-1 group, SA-2 group, SA-3 group). The overall experiment was repeated to minimize the error caused by different batches of animals. Three rats from each group were randomly chosen for the subsequent experiments in both of the trials.

Fundus Imaging

Animals were induced into a coma using isoflurane. A 1% tropicamide solution was applied to the eye to dilate the pupil. Subsequently, the rats were examined using a retinal camera (TRC-50IX, Topcon Medical Systems, Tokyo, Japan). The lens was adjusted to focus on the retina, and images of each rat were then captured.

Blood-Retinal Function Evaluation

After the intravenous injection of EBD (45 mg/kg) through the tail vein, the rat's heart was injected with 100 mL PBS for 1 h. The eyes were collected after the rats were treated with excess isoflurane. Samples were then extracted for grinding, ultrasound, and centrifugation (12,000 ×g, 30 min, 4 °C). The supernatant was collected, and the same amount of 50% trichloroacetic acid was added for every 200 μL sample. The samples were incubated overnight at 4 °C and centrifuged again (12,000 ×g, 30 min, 4 °C). A method similar to enzyme-linked immunosorbent assay (ELISA) was used to determine the EBD content at 610 nm in Microplate Reader (PR4100, Bio-Rad Laboratories, Hercules, CA, USA) and quantified according to the standard curve.

Hematoxylin-Eosin (HE) Staining

After the rats were euthanized (the anesthetic was Tiletamine Hydrochloride and Zolazepam Hydrochloride for injection, which was provided by the Animal Experimental Center of Zhejiang Chinese Medicine University according to the animal weight limit, and the anesthetic dosage of rats was 100 g/100 μL. The execution method is cervical dislocation.), their eyes were removed. The samples, which were embedded in paraffin, were sliced into 4 μm sections using 4% paraformaldehyde, decalcified in xylene, and then dehydrated after ethanol treatment. The sections were stained with hematoxylin-eosin, and the tissue was examined under a light microscope (IX83, Olympus, Tokyo, Japan).

CD31-Immunohistochemistry Analysis

The collected retina specimens were fixed, embedded in paraffin, and then cut into 5 μm segments. Subsequently, antigen repair was performed, and endogenous peroxidase activity was reduced by incubating the sections with 2.5% hydrogen peroxide methanol solution. To reduce nonspecific binding, the tissue sections were incubated with 10% normal goat serum. Anti-CD31 (1:100) was incubated overnight at 4 °C. Next day, the slices were treated with an all-purpose protein block (Dako) at room temperature for 25 min. The sections were then developed by DAB (Dako) and observed under a light microscope. Subsequently, the sections were counterstained with hematoxylin. Finally, the sections were dehydrated with gradient ethanol, sealed with neutral glue, and examined under a microscope. The brown color represents the staining of CD31.

ROS, MDA, GSH, and IGF1 Content Test

In the *in vivo* study, the eyeballs of the rats were removed to conduct ELISA experiments following the instructions. The concentrations of IGF1, MDA and GSH in the rats were assessed and analyzed. Additionally, the primary retinal cells of mice were extracted, and ROS was detected according to the instructions. All the experiments were performed using a microplate reader, the standard curve was designed and the corresponding results were calculated.

Western Blotting

The protein from the rat eyeball was extracted and quantitatively analyzed using the Bicinchoninic Acid (BCA) Assay. Subsequently, the protein was separated by 30 μg polyacrylamide gel electrophoresis using sodium dodecyl sulfate and transferred to a polyvinylidene fluoride (PVDF) membrane. A 5% solution of BSA was dissolved in TBST and used to incubate the membrane at room temperature for 2 h. The AGE-RAGE signaling pathway was detected by analyzing AGE, RAGE, p-JAK, and p-STAT3 protein changes. The DR-related factors VEGF and TNF-α were also detected. Anti-AGE (1:1000 dilution), anti-RAGE (1:2000), anti-P-JAK (1:1000), anti-P-STAT3 (1:1000), anti-VEGF (1:1000), and anti-TNF-α (1:1000) were incubated at 4 °C overnight. β-actin served as the control group. The corresponding horseradish peroxidase labeled secondary antibody was added to the membrane and incubated at room temperature for 2 h. SuperSignal® West Dura Extended Duration Substrate was used to prepare about 1 mL of ECL working liquid according to the instructions. The transfer film was incubated at room temperature for 1 min, then excess ECL reagents were removed and sealed with plastic wrap. X-ray film is placed in the cassette and exposed about 5 for development and fixing. The relative density of the proteins was analyzed using Image J (1.53k, National Institutes of Health, San Diego, CA, USA).

Bioinformatics Analysis

The targets of "diabetic retinopathy" were searched from different disease databases (Such as: GeneCards (https://www.genecards.org/), Online Mendelian Inheritance in Man (OMIM) (https://www.omim.org/) and DisGeneT (https://www.disgenet.org/)). The intersection of the targets was taken for Venn. Then the common targets were entered into the STRING website (https://cn.string-db.org/) for Protein-Protein Interaction Networks (PPI) analysis (Organisms: Homo sapiens; minimum required interaction score: 0.4; max number of interactors to show: no more than 10 interactors). Finally, the results of PPI and Kyoto Encyclopedia of Genes and Genomes (KEGG) enrichment information were obtained.

Journal of
BIOLOGICAL REGULATORS
and Homeostatic Agents

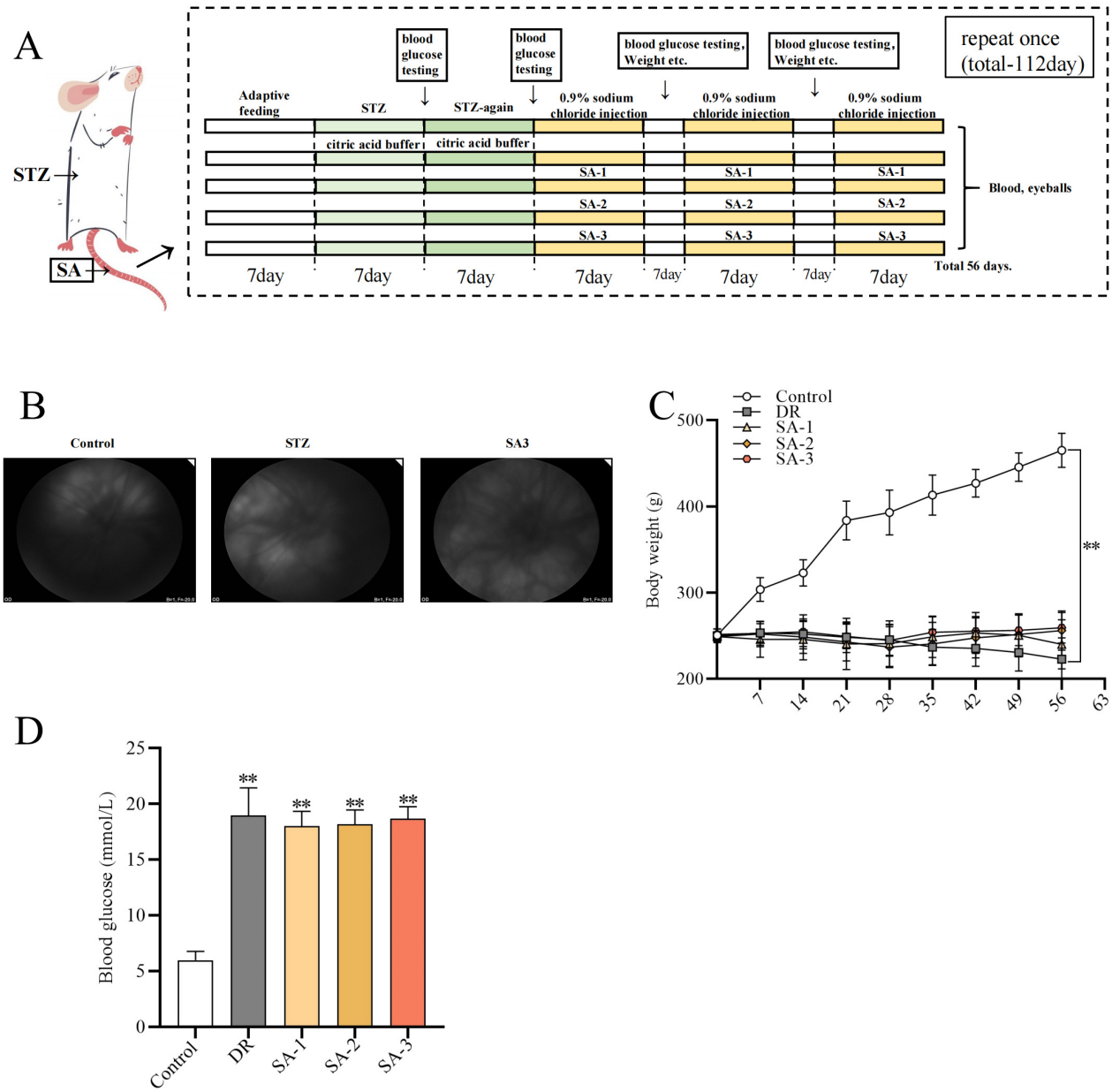

Fig. 1. Information about the rat model of diabetic retinopathy (DR). (A) Overall experimental process. (B) Fundus of rats after the second SA treatment. (C) Recording the weight of each group of rats every 7 days. (D) Blood glucose of each group. $^{**}p < 0.01$ *vs*. control (the mean ± standard deviation (SD), n = 6). One-way Analysis of variance (ANOVA) with Dunnett's post hoc test. STZ, streptozotocin; SA, sodium aescinate.

Statistical Analyses

The experiments were repeated three times, and the mean ± standard deviation (SD) of the data was calculated. Univariate analysis of variance and Tukey post hoc test were used to determine statistical significance. $p < 0.05$ was considered statistically significant. GraphPad Prism software (version: 8.0.1, GraphPad Software, San Diego, CA, USA, https://www.graphpad.com) was used for the analysis.

Results

Effect of SA on SD-Rats Body Weight and Blood Glucose Level

The rats' body weight was recorded every 7 days during the experiment. The total experimental process is shown in Fig. 1A. The diameter of fundus blood vessels was observed in the instrument after each course of treatment (Fig. 1B shows the fundus condition after the second course of SA-3 treatment showed some improvement but no significant improvement). The rats in the DR Group had a significantly lower body weight compared to the control

group ($p < 0.05$). However, the SA treatment group showed no significant effect on weight levels compared to the DR group (Fig. 1C). At the end of the experiment, the changes in blood glucose were measured. The rats in the DR group exhibited hyperglycemia compared to the control group ($p < 0.05$), while the SA treatment group showed no significant effect on blood sugar levels compared to the DR group (Fig. 1D).

Effect of SA on Retinal Vascular Permeability and New Formation

The EBD test was used to assess the impact of SA on retinal vascular permeability. EBD extravasation significantly increased in the DR group ($p < 0.01$). Compared to the DR group, SA could reduce retinal intravascular EBD extravasation in diabetic rats ($p < 0.05$) (Fig. 2). In addition, SA can also affect the formation of blood vessels. According to the immunohistochemical staining results of CD31, the number of CD31 staining increased after STZ intervention compared to the control group, and the production of CD31 decreased after SA treatment, showing a dose-dependent pattern (Fig. 3A,B).

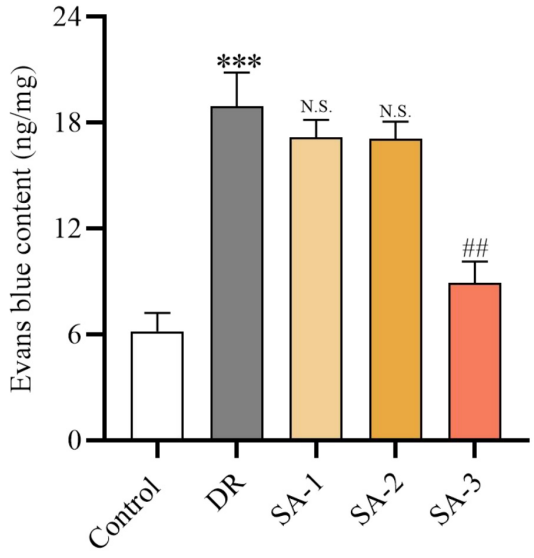

Fig. 2. Intervention effect of SA on vascular permeability. ***$p < 0.001$ *vs.* control, N.S. $p > 0.05$, ##$p < 0.01$ *vs.* DR group (the mean ± standard deviation (SD), n = 6). One-way ANOVA with Dunnett's post hoc test.

SA Effect on Retinal Vessel Diameter and Results of Fundus Photography

The diameter of retinal vessels was significantly greater in the DR group compared to the control group. Micro-angiogenesis was significantly higher than that of control group. In contrast, the diameter of retinal vessels in rats treated with SA was narrowed and micro-vascular reduction compared to the DR group. In addition, fundus bleeding was observed in the STZ model group compared to the control group without intervention, and the bleeding situation changed after SA treatment (Fig. 4).

The Histopathological Changes in Retinal Vessels Induced by SA in Rats

After the administration of SA (0.5/1.0/1.5 mg/kg), there was a reduction in the enlarged diameter of retinal blood vessels in the DR group. The blood vessel diameter was still observed in the low-dose group (0.5 mg/kg) of SA, although it was lower than in the DR group. This difference was not found in the SA-2 and SA-3 groups (as indicated by the arrow in Fig. 5). Hematoxylin-eosin (HE) staining was utilized to assess the thickness of each retinal layer, and the most representative image was chosen (Fig. 5A). The retinal layers included the outer nuclear layer (ONL), outer plexiform layer (OPL), inner nuclear layer (INL), inner plexiform layer (IPL), and ganglion cell layer (GCL). The retinas of the control rats exhibited well-organized structures. Conversely, the cells of the diabetic rats demonstrated irregular, loosened, and disorganized features. As expected, SA treatment improved the damaged cells in each layer. Furthermore, the thickness of each retinal layer, comprising the outer segment (OS), ONL, OPL, INL, IPL, and GCL, as well as the total retina, was significantly reduced in diabetic rats compared to the controls (Fig. 5B). The treatment group receiving SA-2 and SA-3 showed a certain degree of improvement in the thickness of each retinal layer.

Influence of SA on ROS, MDA, GSH, and IGF1 Levels

The GSH level in the DR group was significantly lower than that in the control group ($p < 0.001$). Compared with the DR group, the retinal GSH level in the SA group was significantly increased ($p < 0.05$) (Fig. 6A). The MDA content in the retina of the DR group was significantly higher than that of the control group ($p < 0.01$). Compared with the DR group, MDA contents were decreased after SA treatment ($p < 0.05$) (Fig. 6B). The DCFH-DA probe was used to detect ROS in living cells extracted from the retina of each group. Compared with the control group, ROS content in the DR group was significantly increased ($p < 0.01$), while SA could inhibit such increase ($p < 0.05$) (Fig. 6C). In the detection of serum IGF1, IGF1 in the DR group was increased ($p < 0.01$), but SA could not suppress this point (Fig. 6D). In the detection of IGF1 protein, the expression of IGF1 protein in the DR group was higher than that in the control group, and SA could reduce IGF1 content ($p < 0.01$) (Fig. 6E).

KEGG Analysis Obtained the Relevant Signal Pathway of the Target

Based on the (Fig. 7A), a search for "diabetic retinopathy" in the GeneCards, OMIM, and DisGeNet

Journal of
BIOLOGICAL REGULATORS
and Homeostatic Agents

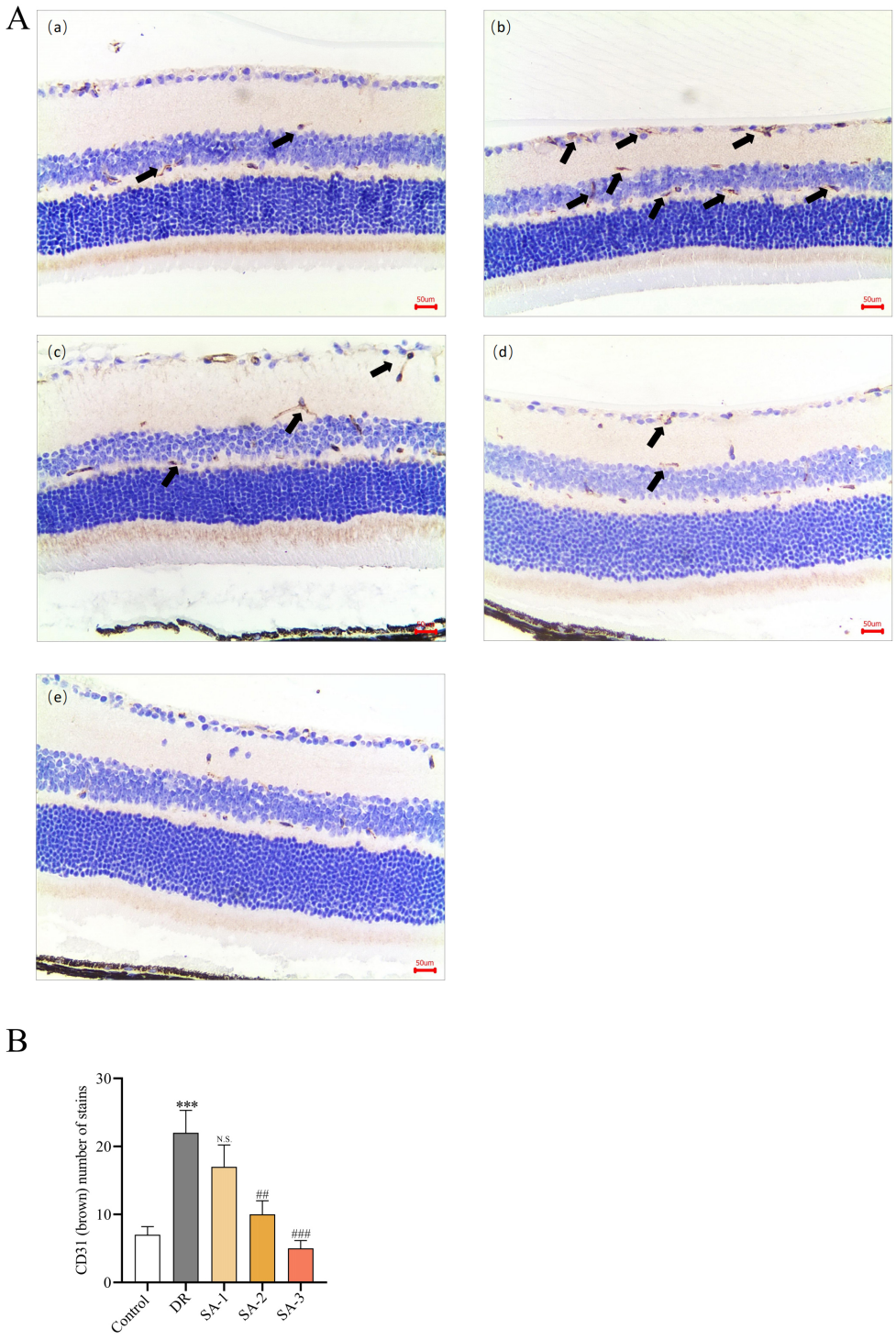

Fig. 3. Effect of SA on Platelet endothelial cell adhesion molecule-1 (CD31) immunohistochemical staining. (A) Typical image of CD31-IHC: (a) control group. (b) DR group. (c) SA (0.5 mg/kg) group. (d) SA (1.0 mg/kg) group. (e) SA (1.5 mg/kg) group. Magnification (×200). Brown is CD31 positive expression, the arrow points to the positive stain. (B) The positive staining was analyzed statistically. ***$p < 0.001$ *vs.* control, N.S. $p > 0.05$, ##$p < 0.01$, ###$p < 0.005$ *vs.* DR group (the mean ± standard deviation (SD), n = 6). One-way ANOVA with Dunnett's post hoc test.

databases resulted in the identification of relevant disease targets (Fig. 7A). Subsequently, 27-targets were input into STRING to build a Protein-Protein Interaction Networks (PPI) (Fig. 7B). Finally, the KEGG enrichment results from STRING were exported, and the top ten relevant signaling pathways were plotted using R language (Fig. 7C).

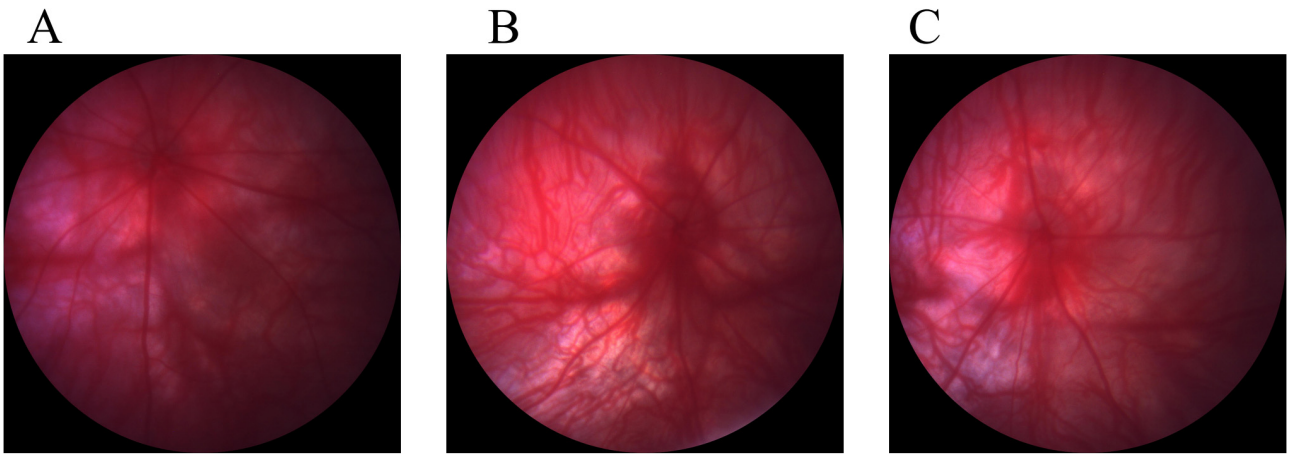

Fig. 4. Fundus imaging in rats. (A) Rats without intervention. (B) Streptozotocin (STZ) was used to construct a DR model in rats. (C) After constructing the DR model of STZ progression, the rats in the SA-high treatment group were treated.

Influence of SA on the AGE-RAGE and Janus Kinase-Signal Transd Ucer and Activator of Transcription 3 (JAK-STAT3) Signaling Pathway

In the AGE-RAGE signaling pathway, compared with the control group, both AGE and RAGE were highly expressed in the DR Group ($p < 0.05$, $p < 0.01$), while JAK and STAT3, downstream of this signaling pathway, did not change. Further analysis of their phosphorylated proteins revealed that P-JAK and P-STAT3 were both increased compared to the control group ($p > 0.05$). However, after SA treatment, the expression of AGE and RAGE decreased, with no significant effect on JAK and STAT3 ($p > 0.05$). Additionally, SA decreased the expression of phosphorylated P-JAK and P-STAT3 ($p < 0.05$, $p < 0.01$) (Fig. 8A–D). These results suggest that SA could inhibit the AGE-RAGE signaling pathway.

Intervention Effect of SA on Related Proteins TNF-α and VEGF

In the DR group, both TNF-α and VEGF were increased compared to the control group. The increase of TNF-α could be inhibited by SA ($p < 0.05$, $p < 0.01$). However, in the case of VEGF, a low dose of SA (0.5, 1.0 mg/kg) could not inhibit the increase in the DR group. When the SA dose was increased to 1.5 mg/mL, VEGF could be effectively inhibited ($p < 0.01$) (Fig. 9A–C).

Discussion

Sodium aescinate (SA) is a commonly used treatment for vascular diseases, particularly cerebrovascular diseases. It primarily improves venous tension, accelerates venous blood flow, promotes lymphatic return, enhances blood circulation and microcirculation, and protects the blood vessel wall. Additionally, it possesses anti-inflammatory and anti-seepage properties. Previous research experiments have employed SA to examine its effects on reducing oxidative stress and inflammation [23,25]. The therapeutic efficacy of SA on micro-vessels has been widely applied in clinical settings, and its impact on ROS and inflammation has been confirmed by previous studies. However, its potential in the treatment of DR has not been explored. In this study, for the first time, it was demonstrated that SA inhibits the production of ROS, alleviates DR *in vivo* by regulating the balance of oxidation, and inhibits the AGE-RAGE (receptor for advanced glycation end products) signaling pathway in STZ-induced DR rats. The findings indicate that although the therapeutic doses of SA (0.5 and 1.0 mg/kg) did not yield significant effects in the CD31 and Evans blue experiments, the treatment group receiving 1.5 mg/kg SA exhibited a clear and significant impact. 1.5 mg/kg SA can decrease the diameter of blood vessels in the fundus of DR rats and reduce the formation of new blood vessels *in vivo*. These results suggest that SA holds promise as a potential therapeutic agent for the treatment of DR. Further research is needed to elucidate the underlying mechanisms and assess its effectiveness in clinical settings.

High glucose levels in individuals with diabetes can impair cellular repair mechanisms over time, which is a key factor in the development of DR [26,27]. The current study revealed that SA treatment (different dose) had a minimal effect on blood glucose levels, suggesting that the observed improvement in STZ-induced DR rats may not be directly associated with the reduction of blood glucose levels ($p > 0.05$). Insulin-like growth factor 1 (IGF1) has been identified as a correlating factor in the progression of DR. The relationship between IGF1 and DR is intricate. Chronic deficiency of IGF1 can lead to retinal capillary degeneration, while a sharp increase in exogenous IGF1 can further enhance the vascular endothelial growth factor (VEGF) and contribute to the progression of DR. In this experiment, the translation level of IGF1 protein increased in the DR group, although the SA-1 and SA-2 dose groups did not significantly regulate the expression of IGF1 protein ($p > 0.05$).

Journal of
BIOLOGICAL REGULATORS
and Homeostatic Agents

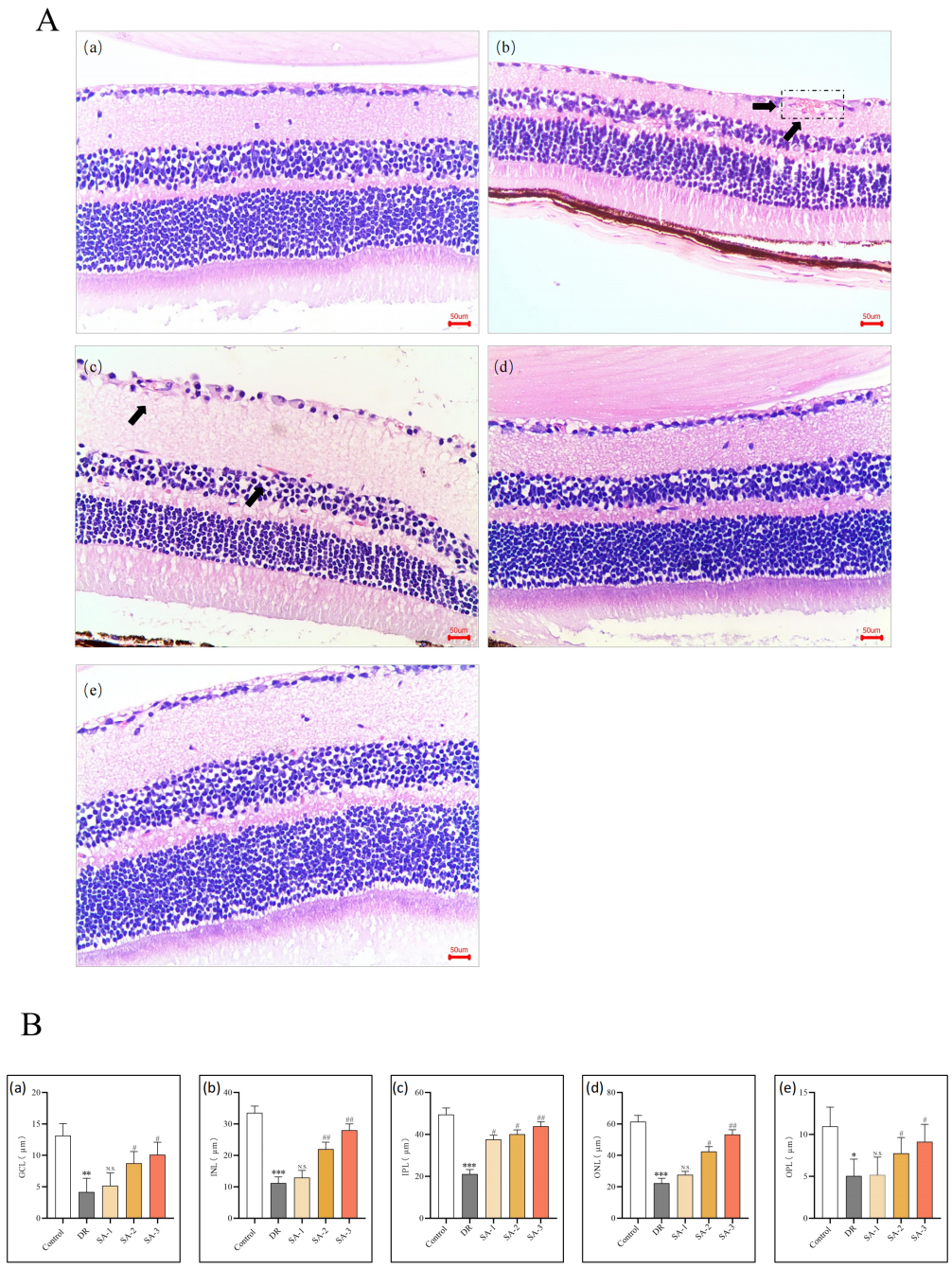

Fig. 5. Retinal damage was observed by HE staining. (A) HE staining image, representing thickness and damage of each layer (×200). (a) Control group, (b) DR-group, (c) SA1-group, (d) SA2-group, (e) SA3-group. Arrows represent possible bleeding spots. (B) Comparison of the thickness of each layer among different groups. (a–e) Thickness levels of ONL, OPL, INL, IPL and GGL. *$p < 0.05$, **$p < 0.01$, ***$p < 0.001$ *vs.* control, N.S. $p > 0.05$, #$p < 0.05$, ##$p < 0.01$ *vs.* DR group (the mean ± standard deviation (SD), n = 6). One-way ANOVA with Dunnett's post hoc test. ONL, outer nuclear layer; OPL, outer plexiform layer; INL, inner nuclear layer; IPL inner plexiform layer; GGL, ganglion cell layer; HE, hematoxylin-eosin.

However, the translation level of IGF1 protein was significantly reduced in the SA-3 group ($p < 0.05$). It is worth noting that any dose of SA had no significant impact on serum IGF1 levels ($p > 0.05$). Nevertheless, SA-3 was able to reduce the expression of IGF1 protein ($p < 0.05$). These findings suggest that the therapeutic effect of SA on STZ-induced DR rats may not only be through its influence on blood glucose levels, but also through its regulation of IGF1 protein expression. Further research is needed to fully understand the mechanisms behind this relationship.

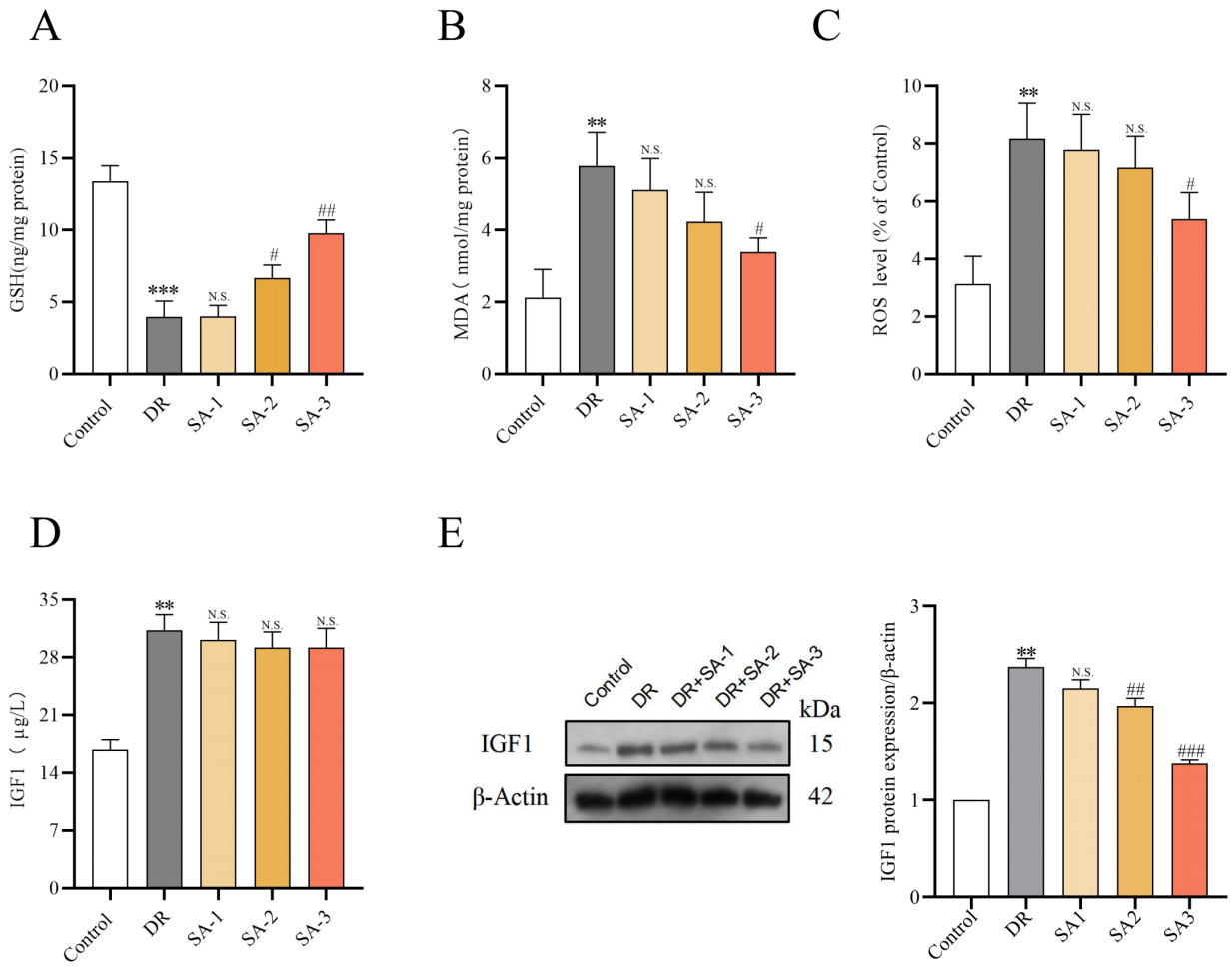

Fig. 6. The effect of SA on oxidative stress-related indexes in Rat cultured with high glucose. (A) Each group results of glutathione (GSH) detection. (B) Each group results of malondialdehyde (MDA) detection. (C) Each group results of reactive oxygen species (ROS) detection. (D) Each group Results of insulin-like growth factor 1 (IGF1) detection in serum of rats. (E) IGF1 western blotting results and quantitative statistics. $^{**}p < 0.01$, $^{***}p < 0.001$ *vs*. control, N.S. $p > 0.05$, $\#p < 0.05$, $\#\#p < 0.01$ *vs*. DR group (the mean ± standard deviation (SD), n = 6). One-way ANOVA with Dunnett's post hoc test.

Diabetic retinopathy (DR) is a complication of diabetes that affects more than one-third of diabetic patients. It is characterized by the development of abnormal neovascularization in the retina. In the early stages, there is microvascular dilation and damage to the blood-retinal barrier, leading to increased retinal vascular permeability, retinal thickening, and edema. During the proliferative period, abnormal proliferation of new blood vessels occurs [28]. The treatment of DR primarily targets the changes and permeability of microvessels, with a strong correlation between VEGF signaling, neovascularization, and persistent ROS signaling [29]. ROS is believed to play a significant role in the occurrence and progression of DR [30]. Regulating ROS through drug intervention is a promising approach in the treatment of DR. The present study showed that in DR rats, there was a significant increase in retinal vessel diameter and extravasation of Evans blue dye (EBD). Consistent with fundus imaging results, histopathology revealed increased retinal vessel diameter due to diabetes. However, treatment with SA alleviated pathological changes caused by hyperglycemia. After SA treatment, the diameter and permeability of retinal blood vessels decreased, and histopathological staining showed some improvement in regenerated blood vessels. These findings suggest that SA can reduce the burden of DR in STZ-induced diabetic rats. VEGF and TNF-α are key factors strongly associated with the progression of DR. VEGF, in particular, is targeted as the first-line treatment for DR [31]. The most recent research shows a strong link between VEGF and ROS [32]. TNF-α also plays a role in the DR process by inducing oxidative damage. The upregulation of these factors acts as a marker for DR progression [33]. The study examined the

Journal of
BIOLOGICAL REGULATORS
and Homeostatic Agents

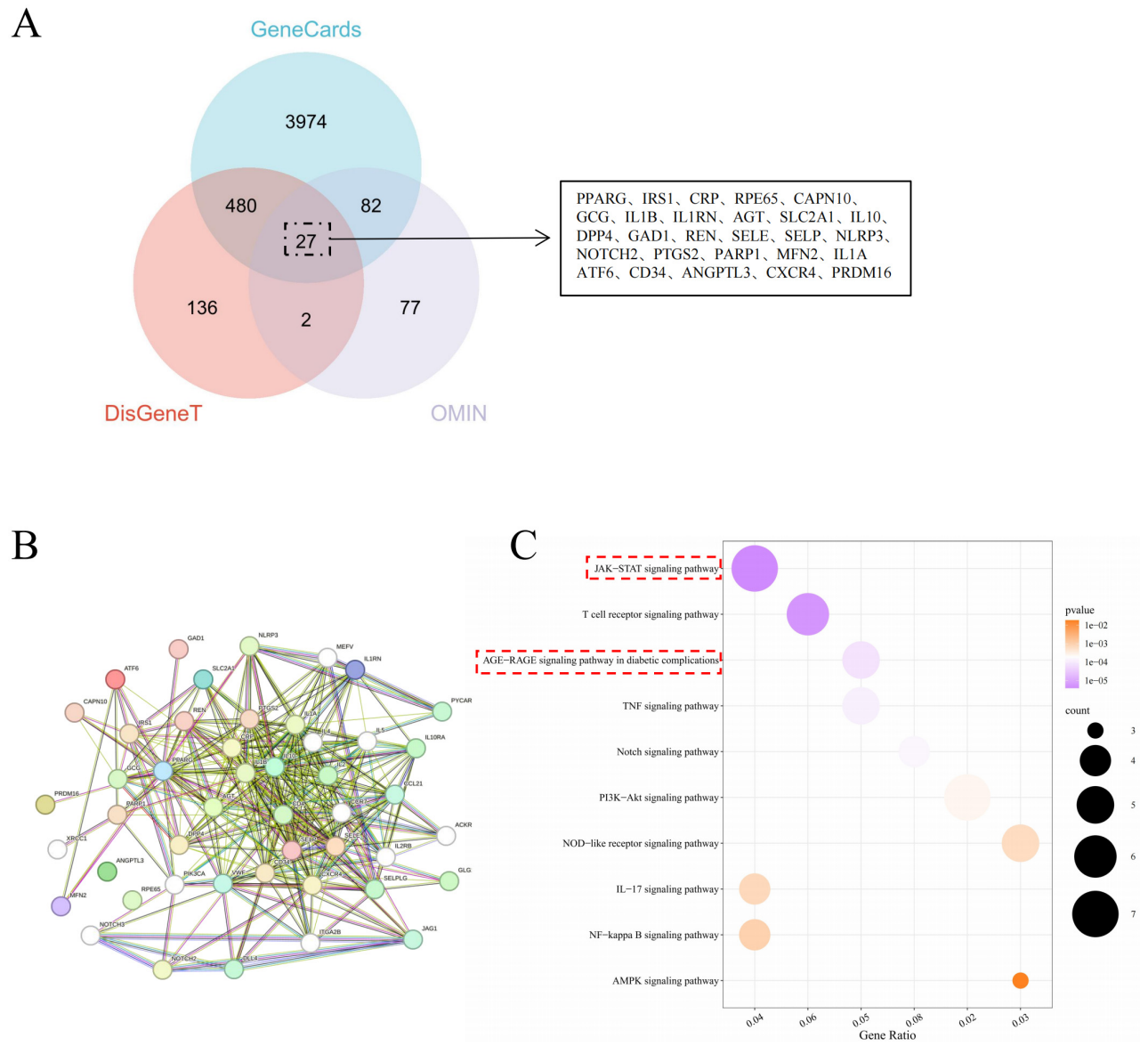

Fig. 7. DR Targets were obtained and Protein-Protein Interaction Networks (PPI) and Kyoto Encyclopedia of Genes and Genomes (KEGG) analysis results were obtained. (A) DR Related targets obtained from GeneCards, Online Mendelian Inheritance in Man (OMIM), and DisGenT databases. (B) PPI analysis results of intersection targets. (C) KEGG enrichment analysis of intersection targets.

effect of SA on VEGF and found that its expression was significantly enhanced in the DR group compared to the control group ($p < 0.005$). However, with the administration of SA (1.5 mg/kg), the expression of VEGF and TNF-α was down-regulated compared to the DR group. Additionally, markers of oxidative stress, MDA and GSH, were examined. MDA levels increased in the model group but decreased in the SA-2 (1.0 mg/kg) and SA-3 (1.5 mg/kg) intervention group ($p < 0.05$). GSH levels decreased in the model group but increased after SA-3 intervention ($p < 0.05$, $p < 0.01$). The DCFH-DA probe was used to detect changes in ROS levels in primary ocular cells. The results indicated higher ROS levels in the DR group compared to the control group ($p < 0.05$). However, treatment with SA-3 reduced ROS expression compared to the DR group ($p < 0.05$). These findings suggest that SA may alleviate DR by intervening in ROS levels. There was no gradient dependence of SA on oxidative stress related indexes. Therefore, SA-3 (1.5 mg/kg) shows promise as a therapeutic intervention for DR by targeting microvascular changes, modulating VEGF and TNF-α expression, and reducing oxidative stress and ROS levels. Further research is needed to explore the full potential and mechanisms of SA in DR treatment.

In previous studies, it has been observed that ROS can increase the expression of muscle-advanced glycation end products (AGEs) and activate their receptor RAGE, leading to retinal damage and the promotion of a pro-inflammatory environment characterized by oxidative stress [34,35]. The formation and accumulation of AGEs are significant factors in the pathogenesis of diabetic retinopathy (DR) and play a

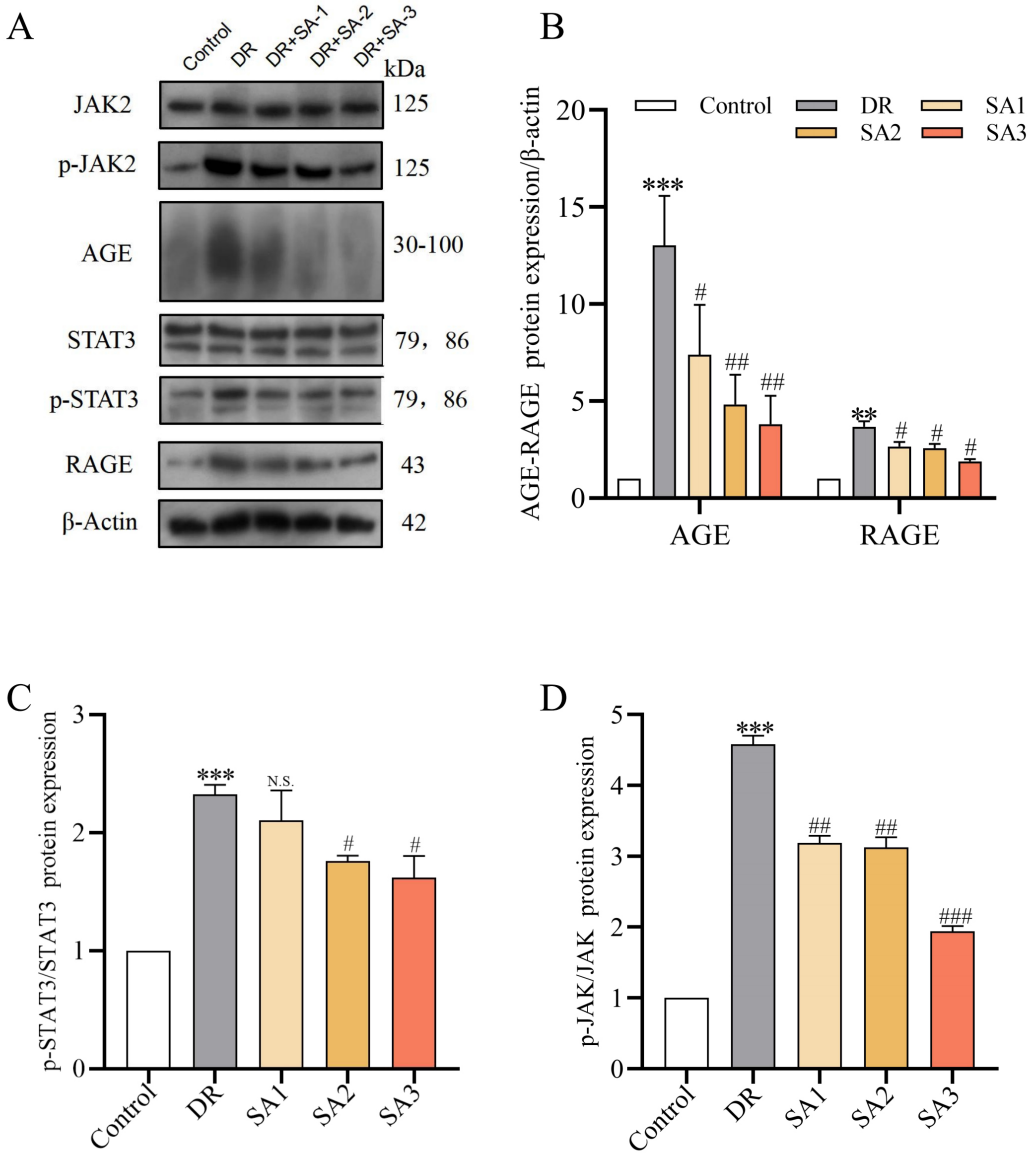

Fig. 8. Effect of SA on advanced glycation end products (AGE)-receptor for AGEs (RAGE) and Janus kinase-signal transd ucer and activator of transcription 3 (JAK/STAT3) signaling pathway. (A) Developed images by western blotting from AGE-RAGE. (B) Histogram of quantitative analysis of AGE, RAGE protein. (C) p-STAT3 protein quantitative analysis column diagram, compared with STAT3. (D) Phosphorylation-Janus kinase (p-JAK) protein quantitative analysis column diagram, compared with JAK. ***$p < 0.001$ *vs*. control, N.S. $p > 0.05$, #$p < 0.05$, ##$p < 0.01$ *vs*. DR group (the mean ± standard deviation (SD), n = 6). One-way ANOVA with Dunnett's post hoc test.

crucial role in retinal damage. Inhibiting the AGE-RAGE system is effective in the treatment of DR, making it an important target for intervention [36]. It is an important remission in the development of DR and an important part of the inhibition that drugs can intervene in [37]. In this study, it was found that in the DR group, AGE and RAGE were activated, and a low dose of SA (0.5 mg/kg) had no significant effect on their levels ($p > 0.05$). However, the high dose of SA (1.5 mg/kg) effectively inhibited the AGE content and RAGE activation. Further investigation based on the AGE-RAGE signaling axis from the KEGG official website and previous bioinformatics studies on diabetes complications suggested that the JAK/STAT3 pathway downstream of AGE-RAGE may be correlated with the development of DR [38]. In the KEGG enrichment analysis of DR targets in this study, both the JAK/STAT signaling pathway and the AGE-RAGE signaling pathway were among the top three pathways with the strongest correlation. The evaluation of the role of SA in the AGE-RAGE signaling pathway in this study indicates that different doses of SA

Journal of
BIOLOGICAL REGULATORS
and Homeostatic Agents

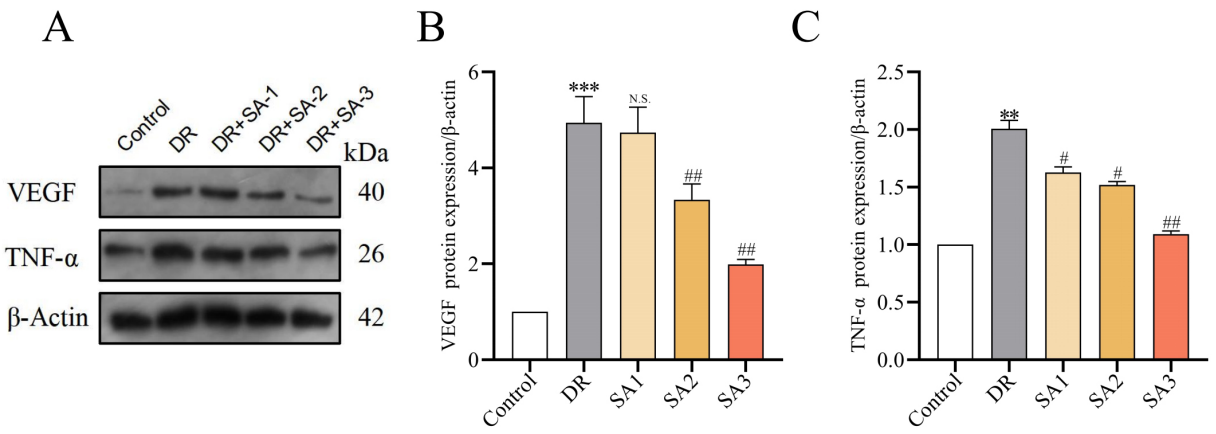

Fig. 9. Changes of IGF1, tumor necrosis factor-α (TNF-α) and vascular endothelial growth factor (VEGF) proteins in SA. (A) Western blotting imaging of IGF1, TNF-α and VEGF. (B,C) Quantitative analysis of IGF1 protein or VEGF protein. $^{**}p < 0.01$, $^{***}p < 0.001$ *vs*. control, N.S. $p > 0.05$, $\#p < 0.05$, $\#\#p < 0.01$ *vs*. DR group (the mean ± standard deviation (SD), n = 6). One-way ANOVA with Dunnett's post hoc test.

can all inhibit the protein expression of AGE and RAGE in the AGE-RAGE signaling pathway. In the downstream JAK/STAT3 signaling pathway, while the total protein levels of JAK and STAT3 remain unchanged, the phosphorylation levels of JAK are influenced by different doses of SA ($p < 0.05$), and the phosphorylation levels of STAT3 are affected by SA-2 and SA-3 ($p < 0.05$), with no significant impact from SA-1 ($p > 0.05$). Both SA-2 and SA-3 inhibit the overexpression of DR-induced p-JAK and p-STAT3, suggesting that SA may alleviate DR by modulating the AGE-RAGE and JAK-STAT3 signaling pathways.

This study has several limitations. For instance, although the selection of animals took into account the different batches, only female rats were chosen, and no research or discussion on gender was conducted. Additionally, there was no investigation into the potential toxicity of SA; the focus was solely on the efficacy of SA for DR, which is an area for improvement in future experiments. Furthermore, due to limited research on the treatment of DR with SA, we only conducted validation on the most strongly correlated AGE-RAGE and JAK/STAT3 signaling pathways and other related factors such as IGF1, TNF-α, and VEGF, based on bioinformatics analysis and literature searches related to DR. Reverse validation of the signaling pathways was not conducted, and other pathways were not studied. SA is not a commonly used drug for the clinical treatment of DR. Clinical treatment for DR largely involves controlling blood pressure, blood sugar, and laser photocoagulation therapy. Subsequent clinical research on the use of SA should consider comparative or collaborative studies in relevant clinical treatments for DR.

Conclusions

Overall, these findings provide insights into the potential mechanisms through which SA exerts its beneficial effects in DR, specifically by targeting the AGE-RAGE and the JAK/STAT3 signaling pathway. Further research will fully elucidate the underlying mechanisms and therapeutic potential of SA in the management of DR.

Availability of Data and Materials

The data used to support the study are available from the corresponding author upon request.

Author Contributions

SLJ designed and performed the research, analyzed the data. YC supervised the experimental process and reviewed the manuscript of the final version. YC was involved in the design of the project, writing and critically revising the manuscript. SLJ and YC has been involved in drafting the manuscript and both authors have been involved in revising it critically for important intellectual content. Both authors read and approved the final manuscript. Both authors have participated sufficiently in the work and agreed to be accountable for all aspects of the work.

Ethics Approval and Consent to Participate

The animal study was approved by the Ethics Committee for Animal Study in Animal Ethical and Welfare Committee of Zhejiang Chinese Medical University (approval number: IACUC-20230904-04).

Acknowledgment

Not applicable.

Funding

The financial support for this manuscript is: Zhejiang Province Traditional Chinese Medicine Science and Technology Project (No.2023ZL418).

Conflict of Interest

The authors declare no conflict of interest.

References

[1] Zhang X, Sivaprasad S, Ting DSW. Editorial: Ocular complications associated with diabetes mellitus. Frontiers in Endocrinology. 2023; 14: 1193522.
[2] Simó R, Hernández C. New Insights into Treating Early and Advanced Stage Diabetic Retinopathy. International Journal of Molecular Sciences. 2022; 23: 8513.
[3] Chaudhary S, Zaveri J, Becker N. Proliferative diabetic retinopathy (PDR). Disease-a-Month. 2021; 67: 101140.
[4] Danek D, Larsen B, Anderson-Nelson S. Non-proliferative diabetic retinopathy. Disease-a-Month. 2021; 67: 101139.
[5] Cheung N, Mitchell P, Wong TY. Diabetic retinopathy. Lancet. 2010; 376: 124–136.
[6] Durham JT, Herman IM. Microvascular modifications in diabetic retinopathy. Current Diabetes Reports. 2011; 11: 253–264.
[7] Antonetti DA, Silva PS, Stitt AW. Current understanding of the molecular and cellular pathology of diabetic retinopathy. Nature Reviews. Endocrinology. 2021; 17: 195–206.
[8] Iwona BS. Growth Factors in the Pathogenesis of Retinal Neurodegeneration in Diabetes Mellitus. Current Neuropharmacology. 2016; 14: 792–804.
[9] Wang Z, Xiong L, Wang G, Wan W, Zhong C, Zu H. Insulin-like growth factor-1 protects SH-SY5Y cells against β-amyloid-induced apoptosis via the PI3K/Akt-Nrf2 pathway. Experimental Gerontology. 2017; 87: 23–32.
[10] Ushio-Fukai M. VEGF signaling through NADPH oxidase-derived ROS. Antioxidants & Redox Signaling. 2007; 9: 731–739.
[11] Zou J, Fei Q, Xiao H, Wang H, Liu K, Liu M, *et al*. VEGF-A promotes angiogenesis after acute myocardial infarction through increasing ROS production and enhancing ER stress-mediated autophagy. Journal of Cellular Physiology. 2019; 234: 17690–17703.
[12] Al-Kharashi AS. Role of oxidative stress, inflammation, hypoxia and angiogenesis in the development of diabetic retinopathy. Saudi Journal of Ophthalmology. 2018; 32: 318–323.
[13] Mukai E, Fujimoto S, Inagaki N. Role of Reactive Oxygen Species in Glucose Metabolism Disorder in Diabetic Pancreatic β-Cells. Biomolecules. 2022; 12: 1228.
[14] Rizwan H, Pal S, Sabnam S, Pal A. High glucose augments ROS generation regulates mitochondrial dysfunction and apoptosis via stress signalling cascades in keratinocytes. Life Sciences. 2020; 241: 117148.
[15] Zhang Z, Huang Q, Zhao D, Lian F, Li X, Qi W. The impact of oxidative stress-induced mitochondrial dysfunction on diabetic microvascular complications. Frontiers in Endocrinology. 2023; 14: 1112363.
[16] Walke PB, Bansode SB, More NP, Chaurasiya AH, Joshi RS, Kulkarni MJ. Molecular investigation of glycated insulin-induced insulin resistance via insulin signaling and AGE-RAGE axis. Biochimica et Biophysica Acta. Molecular Basis of Disease. 2021; 1867: 166029.
[17] Mohd Nor NA, Budin SB, Zainalabidin S, Jalil J, Sapian S, Jubaidi FF, *et al*. The Role of Polyphenol in Modulating Associated Genes in Diabetes-Induced Vascular Disorders. International Journal of Molecular Sciences. 2022; 23: 6396.
[18] Giacco F, Brownlee M. Oxidative stress and diabetic complications. Circulation Research. 2010; 107: 1058–1070.
[19] Brownlee M. The pathobiology of diabetic complications: a unifying mechanism. Diabetes. 2005; 54: 1615–1625.
[20] Song XH, Wang WH, Chen ST, Chen S, Zhang J, Wang YS, *et al*. Application of high performance liquid-ion trap mass spectrometry in analyzing saponins in sodium aescinate. China Journal of Chinese Materia Medica. 2016; 41: 2449–2454. (In Chinese)
[21] Wang B, Yang R, Ju Q, Liu S, Zhang Y, Ma Y. Clinical effects of joint application of β-sodium aescinate and mannitol in treating early swelling after upper limb trauma surgery. Experimental and Therapeutic Medicine. 2016; 12: 3320–3322.
[22] Wang J, Wang H, Xu H, Li J, Zhang X, Zhang X. Solid lipid nanoparticles as an effective sodium aescinate delivery system: formulation and anti-inflammatory activity. RSC Advances. 2022; 12: 6583–6591.
[23] Wang YK, Han J, Xiong WJ, Yuan QY, Gu YP, Li J, *et al*. Evaluation of in vivo antioxidant and immunity enhancing activities of sodium aescinate injection liquid. Molecules. 2012; 17: 10267–10275.
[24] Kang Q, Yang C. Oxidative stress and diabetic retinopathy: Molecular mechanisms, pathogenetic role and therapeutic implications. Redox Biology. 2020; 37: 101799.
[25] Huang XJ, Wang DG, Ye LC, Li J, Akhtar M, Saleem S, *et al*. Sodium aescinate and its bioactive components induce degranulation via oxidative stress in RBL-2H3 mast cells. Toxicology Research. 2020; 9: 413–424.
[26] Roy S, Kim D, Lim R. Cell-cell communication in diabetic retinopathy. Vision Research. 2017; 139: 115–122.
[27] Bryl A, Mrugacz M, Falkowski M, Zorena K. The Effect of Diet and Lifestyle on the Course of Diabetic Retinopathy-A Review of the Literature. Nutrients. 2022; 14: 1252.
[28] Kohner EM. Diabetic retinopathy. British Medical Journal. 1993; 307: 1195–1199.
[29] Fukai T, Ushio-Fukai M. Cross-Talk between NADPH Oxidase and Mitochondria: Role in ROS Signaling and Angiogenesis. Cells. 2020; 9: 1849.
[30] Volpe CMO, Villar-Delfino PH, Dos Anjos PMF, Nogueira-Machado JA. Cellular death, reactive oxygen species (ROS) and diabetic complications. Cell Death & Disease. 2018; 9: 119.
[31] Kim EJ, Lin WV, Rodriguez SM, Chen A, Loya A, Weng CY. Treatment of Diabetic Macular Edema. Current Diabetes Reports. 2019; 19: 68.
[32] Ma Q, Shen JH, Shen SR, Das UN. Bioactive lipids in pathological retinopathy. Critical Reviews in Food Science and Nutrition. 2014; 54: 1–16.
[33] Chantelau E, Kimmerle R, Meyer-Schwickerath R. Insulin, insulin analogues and diabetic retinopathy. Archives of Physiology and Biochemistry. 2008; 114: 54–62.
[34] Zong H, Ward M, Stitt AW. AGEs, RAGE, and diabetic retinopathy. Current Diabetes Reports. 2011; 11: 244–252.
[35] Chen YH, Chen ZW, Li HM, Yan XF, Feng B. AGE/RAGE-Induced EMP Release via the NOX-Derived ROS Pathway. Journal of Diabetes Research. 2018; 2018: 6823058.
[36] Chen M, Curtis TM, Stitt AW. Advanced glycation end products and diabetic retinopathy. Current Medicinal Chemistry. 2013; 20: 3234–3240.
[37] Koulis C, Watson AMD, Gray SP, Jandeleit-Dahm KA. Linking RAGE and Nox in diabetic micro-and macrovascular complications. Diabetes & Metabolism. 2015; 41: 272–281.
[38] Mahmoudi A, Atkin SL, Nikiforov NG, Sahebkar A. Therapeutic Role of Curcumin in Diabetes: An Analysis Based on Bioinformatic Findings. Nutrients. 2022; 14: 3244.